The Astrophysical Journal, 732:85 (7pp), 2011 May 10 doi:10.1088/0004-637X/732/2/85

SUPERMODEL ANALYSIS OF THE HARD X-RAY EXCESS IN THE COMA CLUSTER

R. Fusco-Femiano[1], M. Orlandini[2], M. Bonamente[3,4], and A. Lapi[5,6]

[1] INAF/IASF-Roma, Via del Fosso del Cavaliere, I-00133 Roma, Italy

[2] INAF/IASF-BO, Via Gobetti 101, I-40129 Bologna, Italy

[3] Department of Physics, University of Alabama, Huntsville, AL 35899, USA

[4] National Space Science and Technology Center, NASA Marshall Space Flight Center, Huntsville, AL 35812, USA

[5] Dipartimento di Fisica, Università "Tor Vergata," Via Ricerca Scientifica 1, I-00133 Roma, Italy

[6] SISSA/ISAS, Via Bonomea 265, I-34136 Trieste, Italy

Received 2010 November 30; accepted 2011 March 4; published 2011 April 20

ABSTRACT

The Supermodel (SM) provides an accurate description of the thermal contribution by the hot intracluster plasma which is crucial for the analysis of the hard excess. In this paper, the thermal emissivity in the Coma cluster is derived starting from the intracluster gas temperature and density profiles obtained by the SM analysis of X-ray observables: the *XMM-Newton* temperature profile and the *ROSAT* brightness distribution. The SM analysis of the *BeppoSAX*/Phoswich Detector System (PDS) hard X-ray (HXR) spectrum confirms our previous results, namely, an excess at the confidence level (c.l.) of $\sim 4.8\sigma$ and a nonthermal (NT) flux of $(1.30 \pm 0.40) \times 10^{-11}$ erg cm^{-2} s^{-1} in the energy range 20–80 keV. A recent joint *XMM-Newton*/*Suzaku* analysis reports an upper limit of $\sim 6 \times 10^{-12}$ erg cm^{-2} s^{-1} in the energy range 20–80 keV for the NT flux with an average gas temperature of 8.45 ± 0.06 keV and an excess of NT radiation at a c.l. above 4σ, without including systematic effects, for an average *XMM-Newton* temperature of 8.2 keV in the *Suzaku*/HXD-PIN FOV, in agreement with our earlier PDS analysis. Here we present a further evidence of the compatibility between the *Suzaku* and *BeppoSAX* spectra, obtained by our SM analysis of the PDS data, when the smaller size of the HXD-PIN FOV and the two different average temperatures derived by *XMM-Newton* and by the joint *XMM-Newton*/*Suzaku* analysis are taken into account. The consistency of the PDS and HXD-PIN spectra reaffirms the presence of an NT component in the HXR spectrum of the Coma cluster. The SM analysis of the PDS data reports an excess at c.l. above 4σ also for the higher average temperature of 8.45 keV thanks to the PDS FOV being considerably greater than the HXD-PIN FOV.

Key words: galaxies: clusters: general – galaxies: clusters: individual (Coma) – intergalactic medium – radiation mechanisms: non-thermal – X-rays: galaxies: clusters

1. INTRODUCTION

The Supermodel (SM) describes the density and temperature profiles when we consider the entropy-modulated equilibrium of the intracluster plasma (ICP) within the potential wells provided by the dominant dark matter (DM). These two components are related not only by their common potential well but also by parallel accretion of surrounding DM and baryons into the cluster volume (Cavaliere et al. 2009).[7]

An analysis of the X-ray brightness and temperature profiles for both cool core (CC) and non cool core (NCC) clusters has been performed in terms of the SM (Cavaliere et al. 2009; Fusco-Femiano et al. 2009, hereafter FFCL09; Lapi et al. 2010). This analysis highlights how simply the SM represents the main dichotomy "CC versus NCC" clusters in terms of a few ICP parameters governing the radial entropy run ($k(r) = T(r)/n(r)^{2/3}$, where $T(r)$ and $n(r)$ are the ICP temperature and density profiles, respectively) and shows how accurately it fits even complex brightness and temperature profiles. This dichotomy can be represented and understood in terms of two physical parameters marking the ICP entropy profile: the central value k_c and the outer slope a. More structured temperature and brightness profiles need an additional, physical parameter r_f marking the extension of the entropy floor.

The SM has shown that the inward decline of the temperature profile $T(r)$ characteristic of CC clusters is a feature of the non-radiative SM equilibrium focusing also on the conditions for a cooling catastrophe that may be stabilized by ICP condensing around and into a central massive galaxy to trigger accretion on the nuclear black hole. The feature common to CC clusters is their low values of $a \leqslant 1$ and their high values of the concentration $c > 4$ that follow from their being old structures. At the other extreme, the NCC clusters appear to be dynamically young structures characterized by high values of a and low concentrations. The central flat brightness profile present in NCC clusters like Coma and A2256 reveals large central injections of energy and entropy deposited in the form of a floor extended out to r_f. The SM challenges the complexity posed by substructures observed in the temperature profiles of A2256 and A644. It gives evidence of the existence of cold regions that are remnants of a previous cool phase partially erased by a merger event. Such cases may be termed as RCCs for remnant of CCs. Recently, the SM analysis (Lapi et al. 2010) of the steep temperature declines in CC clusters at low redshift (A1795 and PKS 0745-191) observed by *Suzaku* requires a progressive flattening of the entropy run starting at $r \gtrsim 0.2$ of the virial radius R in agreement with the reported entropy profiles (Bautz et al. 2009; George et al. 2009). Lapi et al. (2010) argue that the entropy production at the cluster boundary is reduced or terminated as the accretion rates of DM and intergalactic gas peter out. This weakening of the accretion shocks demands turbulence to develop also in the outskirts of relaxed clusters (Cavaliere et al. 2011).

BeppoSAX detected the presence of nonthermal (NT) radiation in excess of the thermal ICP emission in the Coma cluster (Fusco-Femiano et al. 1999, 2004) and A2256 (Fusco-Femiano

[7] The interested reader may try for her/himself to use the fast SM algorithm made available at the Web site http://people.sissa.it/~lapi/Supermodel/.

et al. 2000, 2005). This evidence has been claimed also by *RXTE* observations (Rephaeli et al. 1999; Rephaeli & Gruber 2002, 2003) reporting NT fluxes in the 20–80 keV energy band in agreement with the *BeppoSAX* values. The Phoswich Detector System (PDS) on board *BeppoSAX* was a suitable instrument to detect NT radiation in galaxy clusters. Since clusters are very weak sources at hard X-ray (HXR) energies above 15 keV, a correct determination of the background is crucial. Thanks to the rocking technique, the PDS was able to perform a background measurement simultaneously with the observations and therefore no modeling of the background was necessary, as is required for other detectors. Moreover, the background was very stable and low for the equatorial orbit of *BeppoSAX*.

For the Coma cluster the PDS analysis has been challenged by the analysis of Rossetti & Molendi (2004, hereafter RM04) with a different software package (SAXDAS) instead of XAS. Fusco-Femiano et al. (2007, hereafter FFLO07) have demonstrated that the use of the SAXDAS package allows one to obtain the same results as the previous analysis with XAS (Fusco-Femiano et al. 2004, hereafter FF04). The main reason for the discrepancy between the two analyses is in the non-accurate selection of the events by RM04 and not in the treatment of the total background as reported by Wik et al. (2011). In particular, an incorrect handling of spurious spikes due to environmental background, when present, introduces noise that enlarges the error bars hiding the presence of an NT excess over the thermal radiation. In fact, FFLO07 show that the confidence level (c.l.) of the excess increases from 2.9σ to 4.2σ when the same time windows of XAS analysis are considered in SAXDAS. Unfortunately, this important point is not reported in the review of Rephaeli et al. (2008). Additional differences between the two analyses that lead to a c.l. of 4.8σ for the excess and the remarks, including the systematic effects, reported in RM04 are amply discussed in FFLO07. Moreover, we underline that the consistency of the cosmic HXR background measured by *BeppoSAX*/PDS (Frontera et al. 2007) with the spectrum observed by the *International Gamma-Ray Astrophysics Laboratory* (*INTEGRAL*; Churazov et al. 2007; Bisnovatyi-Kogan & Pozanenko 2011) and *Swift* (Ajello et al. 2008), all comparable with the historic HEAO-1 measurements (Gruber et al. 1999), implies negligible PDS systematic effects as reported in FFLO07 and Frontera et al. (2007). The correctness of the PDS analyses is also evidenced by the agreement between the *BeppoSAX*/PDS and *Suzaku*/HXD-PIN spectra for the cluster A3667 (Fusco-Femiano et al. 2001; Nakazawa et al. 2009).

Suzaku observations (Wik et al. 2009, hereafter W09) constrain the thermal component by the hot ICP using a joint *XMM-Newton* and *Suzaku*/HXD-PIN analysis reporting an upper limit of $\sim 6 \times 10^{-12}$ erg cm^{-2} s^{-1} in the energy range 20–80 keV for the NT emission with an average temperature of 8.45 ± 0.06 keV. Also, they found an excess at c.l. above 4σ with an annular *XMM-Newton* best-fit value of 8.2 keV in the *Suzaku*/HXD-PIN FOV, in agreement with the results of FF04. For the lower temperature, W09 do not report the NT flux value that this SM analysis indicates to be ∼20% lower than the PDS NT flux here reported for the smaller HXD-PIN FOV than the PDS FOV (see Sections 2 and 3).

With our SM analysis we will show that the marginal evidence of an NT component in the *Suzaku* observations is due to two combined causes: loss of NT flux for the smaller field of view (FOV) of the HXD-PIN with respect to the *BeppoSAX*/PDS and *RXTE* FOVs, and higher average temperature derived by the joint analysis.

The Coma cluster has also been observed by *INTEGRAL* (Eckert et al. 2007; Lutovinov et al. 2008) and *Swift*/BAT (Ajello et al. 2009). Eckert et al. (2007) explore the morphology of the cluster in the HXR energy range 18–30 keV with a deep observation. The *INTEGRAL* image is displaced in the direction of the NGC 4839 group which is merging with the main cluster. They associate the HXR excess in this region with emission from a very hot region of the cluster ($T \geqslant 10$ keV) showed by Neumann et al. (2003) in their *XMM-Newton* temperature map.

Combining data from *INTEGRAL*, *RXTE*, and *ROSAT* observatories, Lutovinov et al. (2008) find that the thermal spectrum can be modeled with a temperature of 8.2 keV and that the cluster is only marginally detectable ($\sim 1.6\sigma$) in the 44–107 keV energy band by *INTEGRAL*. The 20–80 keV flux of a possible NT component ($(6.0 \pm 8.8) \times 10^{-12}$ erg cm^{-2} s^{-1}) is consistent with the *BeppoSAX* and *RXTE* fluxes. They also exclude, with high significance, that the NT emission reported by *BeppoSAX* and *RXTE* could be due to a single point source.

The *Swift* mission is mainly devoted to detecting and localizing gamma-ray bursts. *Swift*/BAT is a coded-mask telescope optimized for the study of point-like sources and can be used to investigate extended objects only if these are detected as point-like. Coma instead is extended in BAT and part of the source flux is lost in the BAT background. Ajello et al. (2009) treated the Coma cluster as a point-like source considering source emission within a radius of $\sim 10'$ from the BAT centroid. They conclude that the presence of an NT component arising from the cluster outskirts cannot be excluded. More recently, Wik et al. (2011) have tested the possibility that the difference between the *Suzaku*/HXD-PIN upper limit (for $T = 8.45$ keV) and the *BeppoSAX* and *RXTE* NT fluxes may be due to the extent of the inverse Compton (IC) emission. Their joint *XMM-Newton*/*Swift* BAT analysis requires an accurate cross-calibration between the two instruments and to model both the thermal and NT spatial distributions. Moreover, the analysis is characterized by a higher uncertainty than for a point source (Ajello et al. 2009; Wik et al. 2011). The derived upper limits to the NT radiation are inconsistent with the *BeppoSAX* and *RXTE* observations.

In this paper, Section 2 reports the procedure followed for the SM analysis of the HXR PDS spectrum in the Coma cluster. This analysis relies on the ICP density and temperature profiles fixed by the SM analysis (FFCL09) of the *ROSAT* X-ray brightness and *XMM-Newton* temperature distributions. The presence of an NT spectral component in the HXR PDS spectrum is identified by determining in any point of the cluster the thermal ICP emissivity at a given energy. In the previous *BeppoSAX* and *RXTE* analyses, the ICP thermal contribution was estimated considering bremsstrahlung emission for an average temperature in the FOV of the instruments. Sections 3 and 4 are devoted to the discussion and conclusions, respectively.

In our treatment, we adopt a Coma cluster redshift of 0.0232, Hubble constant $H_0 = 70$ km s^{-1} Mpc^{-1}, and quote error bars at the 68% c.l. One arcmin corresponds to 28.12 kpc.

2. SM ANALYSIS OF THE HARD EXCESS

The SM analysis of the Coma cluster (FFCL09) involves the fit to the *XMM-Newton*-projected emission-weighted temperature profile (Snowden et al. 2008) and to the *ROSAT* surface brightness distribution (Mohr et al. 1999; see Figure 1). For this paper, we have performed a slightly different SM analysis of the X-ray brightness profile with respect to that in FFCL09. We imposed the same value of $r_f = 96 \pm 5$ kpc derived by the

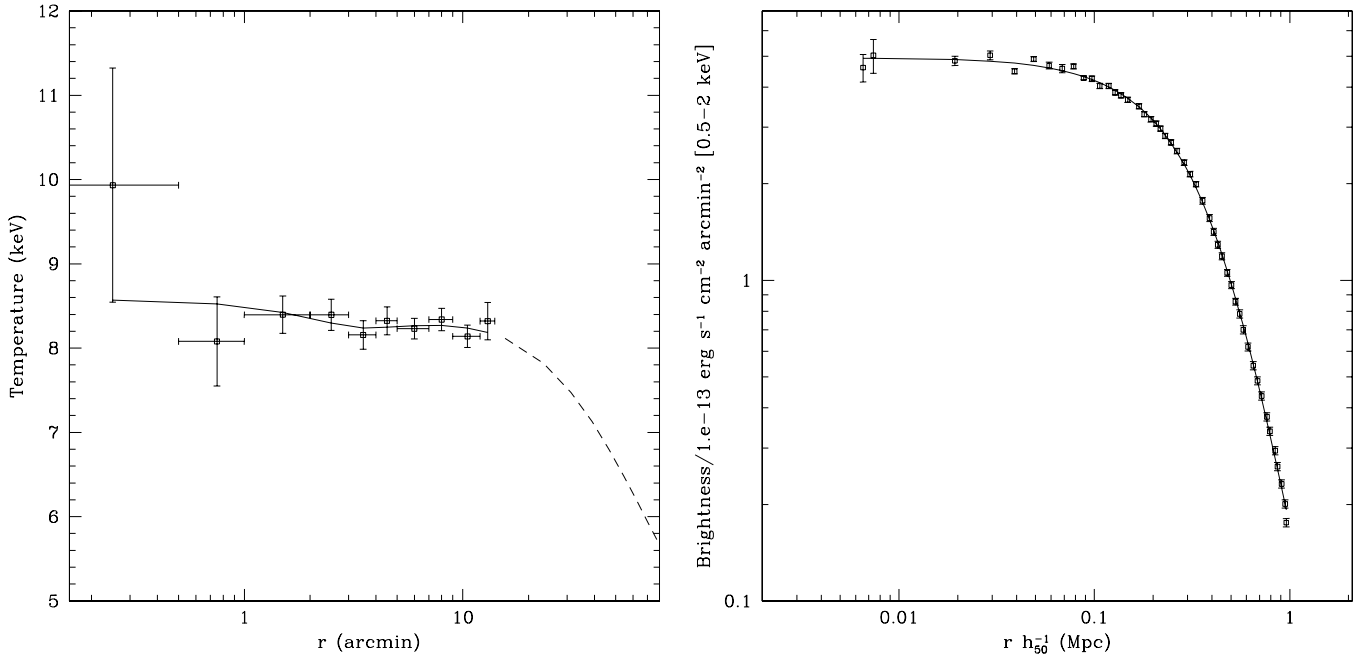

Figure 1. Left panel: projected emission-weighted temperature profile measured by *XMM-Newton* (Snowden et al. 2008). The continuous line represents the SM fit (see FFCL09). The dashed line is the extrapolation of the SM fit to the virial radius R. This profile gives an average temperature of 8.21 ± 0.08 keV (90% c.l.) in the HXD-PIN FOV ($34' \times 34'$), the same value reported by W09 in their *XMM-Newton* analysis of the Coma cluster; right panel: brightness profile in the energy range 0.5–2 keV measured by *ROSAT* (Mohr et al. 1999). The continuous line represents the SM fit ($\chi^2 = 55.5/44$).

temperature profile that obtained a very good fit to the brightness profile (see Figure 1). Instead, an unacceptable χ^2 value is obtained when imposing $r_f = 250^{+44}_{-74}$ kpc, derived by the previous analysis of the brightness profile (see FFCL09), in the fit to the temperature distribution. This implies that the temperature profile is more accurate than the brightness profile in the determination of the entropy floor extension r_f. From this new analysis, we obtain a value of $(4.3 \pm 0.4) \times 10^{-5}$ cm^{-3} for the density at the virial radius R. Thus, the values of r_f and n_R are slightly different from those reported in FFCL09, while the ICP temperature at the virial radius is $T_R = 5.7 \pm 1.0$ keV as reported in FFCL09.

To summarize, the free parameter values that fit the emission-weighted temperature profile of Figure 1 and that determine the temperature and density profiles of Figure 2 are $c = 1.67^{+4.30}$ for the DM and $k_c/k_R = (1.14 \pm 0.83) \times 10^{-1}$, $a = 1.03^{+0.77}$, and $r_f/R = (4.37 \pm 0.23) \times 10^{-2}$ for the ICP. These values fit the *ROSAT* brightness profile (see Figure 1) when they vary within their associated errors. The inverse process that implies that the parameter values should be derived from the brightness profile to fit the temperature distribution is not adequate for the weak dependence of the entropy on the brightness B ($k = T/n^{2/3} \sim T^{7/6}/B^{1/3}$, where $B \sim n^2 T^{1/2}$).

While the use of *ROSAT* data is not justified in the central regions by the PSPC angular resolution ($\sim 25''$) with respect to an *XMM-Newton* profile, at larger radii the latter suffers from a greater total background. Vikhlinin et al. (2006) find an excellent agreement between *Chandra* and *ROSAT* PSPC surface brightness data at large distances where the *ROSAT* data allow us to have a better statistical accuracy.

Several determinations of the virial radius are given in the literature ranging between 2 and 3 Mpc (Castander et al. 2001; Lokas & Mamon 2003; Kubo et al. 2007; Gavazzi et al. 2009). A value of 2.2 Mpc (Gavazzi et al. 2009) has been adopted that corresponds to $78'.24$. The results of the SM analysis (FFCL09) depend only weakly on this choice within one standard deviation.

The profiles of Figure 1 correspond to the temperature and density profiles of Figure 2, with a central temperature of 9.65 keV and central density of 2.5×10^{-3} cm^{-3}. We highlight that the projected emission-weighted temperature SM profile of Figure 1 gives a value of 8.21 ± 0.08 keV (90% c.l.) in the *Suzaku* FOV ($34' \times 34'$), the same value found by W09 in their spectral fits to the *XMM-Newton* regions of the Coma cluster and in agreement with previous measurements. Hughes et al. (1993) derive 8.21 ± 0.16 (90% c.l. and including systematic effects) from *Ginga* over the energy range from 1.5 to 20 keV (collimator 1°–2° FWHM) and Arnaud et al. (2001) report 8.25 ± 0.10 keV (90% c.l.) in the central $r < 10'$ region with the *XMM-Newton*–EPIC-MOS detectors (energy range 0.3–10 keV).

To check the SM extrapolation to the virial radius of the temperature profile represented by the dashed curve of Figure 1, we derive the average temperature within the single collimator with a total square FOV of $65'.5$ on a side considered by W09 to approximate the HXD-PIN spatial response. Our SM value of $\sim$7.85 keV is consistent with the temperature values, reported in Table 1 of W09 in their *XMM-Newton* analysis of the Coma cluster regions, which give an average temperature of 7.79 ± 0.12 keV. This agreement is also visible in Figure 3, which reports the temperature values in the *XMM-Newton* regions R1–R6 investigated by W09 showing a temperature decline consistent with our SM extrapolation up to a distance of more than $30'$ ($\sim 0.4R$) from the cluster center.

To compute the X-ray emission spectrum of the Coma cluster we consider the MEKAL plasma model (Mewe et al. 1985; Mewe et al. 1986; Kaastra & Mewe 1993), the Galactic absorption model (Morrison & McCammon 1983), and the abundance profile $Z(r)$ of Leccardi et al. (2010) for NCC clusters. To take into account the temperature $T(r)$ and density $n(r)$ profiles of Figure 2 in SM analysis of the PDS spectrum,

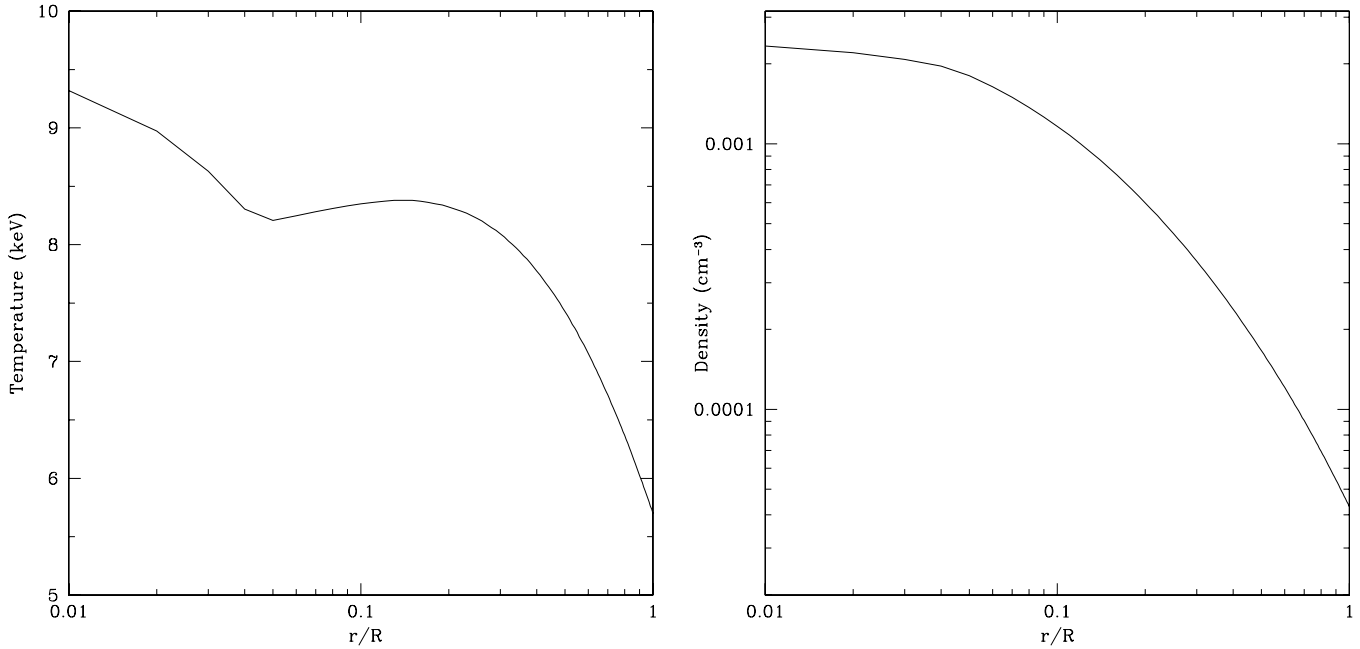

Figure 2. Left panel: temperature profile that fits the projected emission-weighted temperature profile of Figure 1; right panel: density profile that fits the brightness profile of Figure 1.

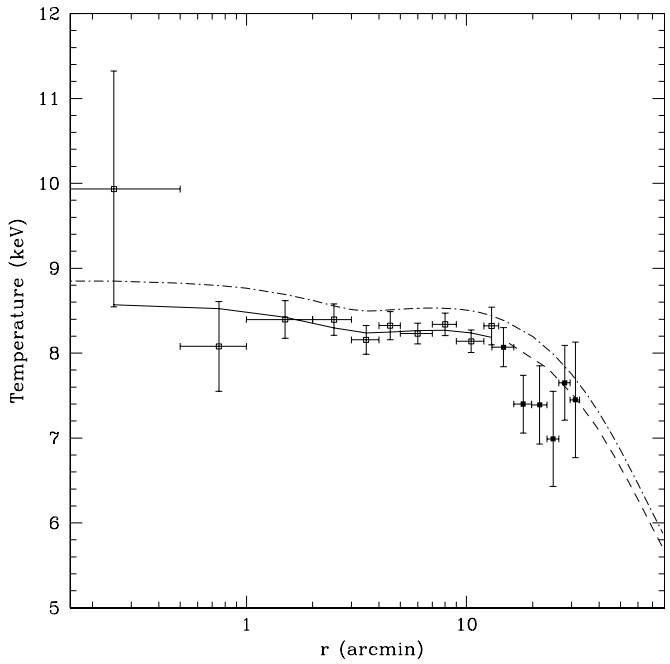

Figure 3. Continuous line represents the SM fit to the *XMM-Newton* temperature profile (empty square points; Snowden et al. 2008) and the dashed line is the SM extrapolation to the virial radius (see Figure 1); the dot-dashed line is the SM fit with an average temperature of 8.45 keV in the HXD-PIN FOV reported by the joint *XMM-Newton*/*Suzaku* analysis (W09). The filled square points are the temperature values in the *XMM-Newton* regions R1–R6 investigated by W09.

we utilize the routine *xsmekl* outside of the *XSPEC* package. At energies above 50 keV where the MEKAL model is undefined we use Equation 1(b) of Mewe et al. (1986) to derive the photon number emissivity at energy E per unit energy interval. The emissivity computed in any point of the cluster $F(E) = n^2(r)\Lambda[T(r), Z(r)]$ in photons cm^{-3} s^{-1} is projected along the line of sight for each energy and then integrated between a spatial interval $(r_1 - r_2)$ always for each energy. Λ is the emissivity derived by *xsmekl*. The Coma cluster flux in photons cm^{-2} s^{-1} represents an additive model that through the command *model atable* in *XSPEC* fits the data.

The ICP temperature and density profiles of Figure 2 determine the cluster thermal emissivity in the energy range 15–80 keV. To compare the SM spectrum with the PDS spectrum (FF04) we have integrated the projected emissivity at a given energy in the full *BeppoSAX* FOV, $r_2 = 78'$ ($r_1 = 0'$). The SM thermal flux at 15 keV is lower by a factor $\sim$1.11 than the PDS flux at the same energy implying an NT excess even at 15 keV. Considering the calibration offset between the *ROSAT*/*XMM-Newton* fit and the *BeppoSAX* data (see Kirsch et al. 2005), we have conservatively normalized the SM thermal spectrum to the PDS flux observed at 15 keV. This requires a slight increase of n_R at $\sim 4.5 \times 10^{-5}$ cm^{-3}, which is within the 1σ uncertainty of the SM determination. After the normalization, we still detect an NT component at $E \geqslant 20$ keV with significance $\sim 4.8\sigma$ with a flux in the energy range 20–80 keV of $(1.30 \pm 0.40) \times 10^{-11}$ erg cm^{-2} s^{-1} for an assumed photon index $\Gamma = 2$ (see Figure 4). The significance and the flux of the NT component are consistent with the previous analysis of FF04 ($\sigma = 4.8$ and flux of $(1.5 \pm 0.5) \times 10^{-11}$ erg cm^{-2} s^{-1}) using an average temperature of 8.11 keV derived by *Ginga* (David et al. 1993). This result is also in agreement with the NT component significance greater than 4σ, without including systematic effects, obtained by *Suzaku* (W09) for $T = 8.2$ keV, the same temperature obtained by the SM for the *Suzaku* FOV (see Figure 1). The NT origin of the hard excess has been verified by fitting the PDS data with a thermal component, instead of a power law, in addition to the SM thermal contribution. The best-fit value for the temperature is $\sim$28.5 keV with a lower limit of $\sim$11.5 keV (90% c.l.) making it unlikely that the hot regions reported by *XMM-Newton* (Neumann et al. 2003) and *INTEGRAL* (Eckert et al. 2007) observations can be responsible for the hard tail detected by *BeppoSAX*/PDS. A recent joint analysis *XMM-Newton*/*Swift* BAT (Wik et al. 2011) has shown inconsistency between the NT upper limits derived for different spatial models with the *BeppoSAX* and *RXTE* detections. We believe that a coded-mask telescope devoted mainly to the study

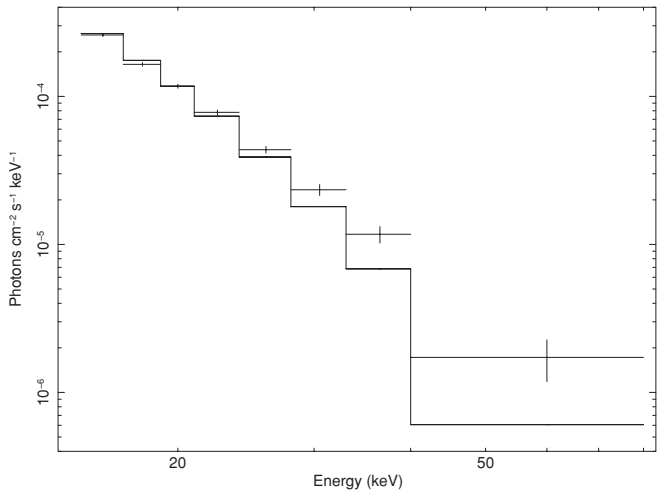

Figure 4. Data representing the HXR spectrum of the Coma cluster observed by *BeppoSAX*/PDS (FF04). The continuous line is the thermal ICP emission derived from the SM analysis using the temperature and density profiles of Figure 2.

of point sources finds several difficulties in disentangling an NT component from the ICP thermal radiation in an extended and weak source at HXR energies like the Coma cluster (see Ajello et al. 2009). Moreover, this analysis requires an accurate cross-calibration between the two detectors.

3. DISCUSSION

Extended radio regions observed in several galaxy clusters, radio halos, and relics provide evidence for the presence of a population of relativistic electrons and magnetic fields in the ICP (see Ferrari et al. 2008). The detection of NT radiation in HXR spectra imposes further constraints to the possible acceleration mechanisms and origin of the relativistic electrons responsible for NT phenomena in galaxy clusters (e.g., Brunetti et al. 2001). The likely origin of the hard excess is IC scattering of relativistic electrons by the cosmic microwave background photons. In this scenario the volume-averaged magnetic field strength and the density of the relativistic electrons can be determined by combining radio and NT X-ray fluxes (Rephaeli 1979). The Coma cluster exhibits a central giant radio halo and a peripheral radio relic with total extent of about $\sim 67'$ at 1.41 GHz with a center $75'$ offset with respect to the X-ray cluster center. Further, the very extended ($\sim 135'$) low surface radio brightness envelope first seen by Kronberg et al. (2007) and confirmed by Brown & Rudnick (2011) could be an additional source for relativistic electrons responsible for the hard IC emission observed by *BeppoSAX* and *RXTE*.

One of the most sensitive points in the search for NT components is the lack of information on the thermal structure of the hot ICP. In the analysis of the non-imaging *BeppoSAX* and *RXTE* observations it was only possible to consider an average temperature in the FOV of the instruments to determine the bremsstrahlung emissivity of the hot gas. While waiting for telescopes able to map the HXR emission and disentangle the thermal and the NT components (such as NuStar[8] and Astro-H[9]), we believe that the SM is a powerful tool to constrain the ICP thermal radiation for a confident assessment of the presence of NT spectral components also in clusters like Coma that shows evidence of ongoing mergers, the hallmark of a recent cluster formation. The extension of the entropy floor, r_f, is interpreted in terms of the stallation radius attained by an outbound blast triggered by a major head-on merger or driven by a violent active galactic nucleus outburst before being degraded into adiabatic sound waves. This interpretation relates r_f to the dating of the merger responsible for the energy/entropy input; the good performance of the SM implies such a time to be intermediate between the blast transit time <0.1 Gyr to reach $r_f \sim 100$ kpc (see Cavaliere & Lapi 2006) and the time of several Gyr needed by radiative cooling to erode the entropy floor. Such a timing guarantees an accurate description of the ICP thermodynamic state by the SM based on hydrostatic equilibrium (for a more detailed discussion see Section 5 of FFCL09). Moreover, the equilibrium of the ICP is somewhat faster to attain than the DM's (see Ricker & Sarazin 2001; Lapi et al. 2005) and the circularized data (integrated over annuli; see Snowden et al. 2008) tend to smooth out local, limited deviations from spherical hydrostatics and to better agree with equilibrium. Conditions of disequilibrium are present in clusters such as the Bullet cluster (see Clowe et al. 2006) or MACS J0025.4-1222 (see Bradač et al. 2008). These conditions, due to stronger if rarer energy injections by deep major mergers, prevent an SM description of the X-ray observables.

The SM allows us to determine the thermal ICP contribution more correctly than the temperature maps that are limited in extension ($\lesssim R/2$), except for a handful of clusters observed by *Suzaku* (Bautz et al. 2009; George et al. 2009; Reiprich et al. 2009; Kawaharada et al. 2010; Hoshino et al. 2010) that does not include Coma, while the *BeppoSAX* FOV extends to $\sim R$. Finally, the accurate SM fit to the brightness profile (see Figure 1) implies that the relevance of the cluster ellipticity is mild.

To show evidence of the presence of an NT feature, we considered the SM ICP temperature and density profiles to derive the underlying contribution of the hot ICP to the HXR Coma spectrum observed by *BeppoSAX*/PDS in the energy range 15–80 keV. The profiles in Figure 2 have been obtained by the SM analysis of the X-ray observables of the Coma cluster: the *XMM-Newton*-projected emission-weighted temperature (Snowden et al. 2008) and the *ROSAT* brightness distribution in the energy range 0.5–2 keV (Mohr et al. 1999). Note that the SM extrapolation of the temperature profile is in agreement with the more recent analysis of the *XMM-Newton* data by W09 up to a distance of $\sim 30'$ from the cluster center (see Figure 3), lending additional support to the use of the SM profiles. A further check of the validity of the SM profiles of Figure 2 is given by the fit to the *ROSAT* PSPC spectrum (energy range 1–2 keV) in the region $20'$–$40'$ around the center of the Coma cluster (Bonamente et al. 2003). The SM spectrum is lower than the *ROSAT* data by only a factor ~ 1.06 (see Figure 5).

The joint *XMM-Newton*/*Suzaku* HXD-PIN analysis (W09) derives a mean temperature of 8.45 keV in the HXD-PIN FOV greater than the temperature used in the *BeppoSAX* and *RXTE* analyses. The authors suggest that the lower temperature may be the effect of the larger FOVs of the two X-ray detectors that include emission from cooler gas in the cluster outskirts. This emission that lowers the average temperature is determined mainly by emission at energies $E < 10$ keV. But a distribution of higher than average temperature regions can increase the average gas temperature observed at high energies. These regions with $T \gtrsim 10$ keV are observed also by *XMM-Newton* (Neumann et al. 2003) and *INTEGRAL* (Eckert et al. 2007).

[8] http://www.nustar.caltech.edu/
[9] http://astro-h.isas.jaxa.jp/

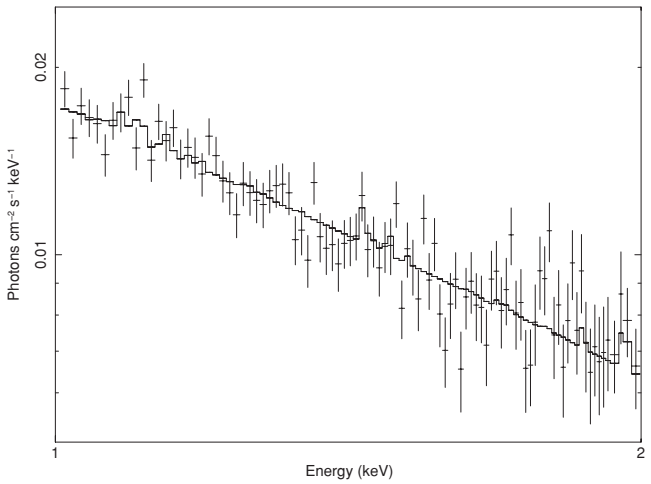

Figure 5. *ROSAT* PSPC spectrum of the 20′–40′ region around the center of the Coma cluster, fitted with the SM profiles of Figure 2 ($\chi^2 = 105.85/99$).

With reference to this interpretation, we note that the value of 8.45 keV in the HXD-PIN implies a temperature run that appears to be in disagreement with the *XMM-Newton* profile (Snowden et al. 2008; W09) as shown by the dot-dashed curve in Figure 3. Moreover, as reported in the introduction a temperature of 8.2 keV has been derived combining data from *INTEGRAL*, *RXTE*, and *ROSAT* (Lutovinov et al. 2008).

An alternative and more likely explanation for the higher temperature value found in the joint *XMM-Newton*/HXD-PIN analysis may be given by the presence of the NT component itself in the spectrum which is responsible for the increase of the average temperature. A power-law component in fact raises the exponential decline of the thermal emission, resulting in a higher best-fit thermal temperature. The poor fit with $T = 8.2$ keV relative to the fit in which the temperature is a free parameter may be indicative of the presence of a second component in the Coma spectrum mainly visible in the energy range covered by the HXD-PIN data.

This SM analysis of the HXR spectrum in the Coma cluster confirms the results of the previous analysis by FF04. However, to remove the possibility that the existence of an NT excess in the HXR spectrum of the Coma cluster may be tied to the ICP average temperature value, we have considered the temperature profile (dot-dashed line in Figure 3) that gives the average temperature of 8.45 keV in the HXD-PIN FOV as reported by W09 in their joint *XMM-Newton*/*Suzaku* analysis. In this case, the PDS spectrum reports a c.l. of $\sim 4.3\sigma$ for the excess and an NT flux of $(1.15 \pm 0.41) \times 10^{-11}$ erg cm^{-2} s^{-1} in the energy range 20–80 keV with $\Gamma = 2$.

We examine also the possibility that the existence of the NT excess may depend on the temperature profile in the spatial range between 30′ and the virial radius ($R = 78.'24$), up to now not covered by observations. To be conservative we have considered a flat temperature profile in this interval with a constant temperature of ~ 7.8 keV, the value at $r = 30' \simeq 0.4R$ (see Figure 2). Although the flattening of the temperature profile seems to be very unlikely (see Figure 3), in this case the excess is at the c.l. of $\sim 4.4\sigma$. Finally, we have considered both these two effects: the higher average temperature of 8.45 keV and the flat temperature profile at $r \geqslant 30'$ with a constant temperature value of ~ 8 keV. Also in these conditions the NT excess does not vanish in the HXR PDS spectrum though at the level of $\sim 3.8\sigma$.

Independently from the real average temperature in the HXD-PIN FOV a relevant point emerges from the analysis of W09. They report that with an *XMM-Newton* average temperature of 8.2 keV, an NT excess with c.l. greater than 4σ is present in the *Suzaku* data, without including systematic effects, assuming a fixed photon index $\Gamma = 2$ for the power-law component. This result, absolutely in agreement with the PDS analysis (FF04), implies that the HXD-PIN spectrum is consistent with the PDS spectrum and therefore in disagreement with the PDS spectrum of RM04 who found a very marginal c.l. for the excess using the same temperature (8.21 keV) and without considering systematic effects.

We also address the agreement between the *Suzaku* and *BeppoSAX* spectra with the following tests.

1. We consider the smaller FOV of *Suzaku* HXD-PIN with respect to that of the PDS and temperature profile for an average $T = 8.2$ keV (continuous and dashed lines in Figure 1); in this case, we obtain an NT flux in the 20–80 keV energy band of $(1.05 \pm 0.41) \times 10^{-11}$ erg cm^{-2} s^{-1} which is $\sim 20\%$ lower than the PDS NT flux of $(1.30 \pm 0.40) \times 10^{-11}$ erg cm^{-2} s^{-1} (see Section 2). The exclusion of part of the cooler cluster regions due to the smaller HXD-PIN FOV reduces the ICP contribution to the thermal emission mainly at energies around 15 keV. This determines a flatter ICP thermal spectrum and thus a lower NT excess that is at a c.l. of $\sim 4\sigma$ in agreement with the W09 analysis.
2. We use the *Suzaku* FOV and temperature profile that gives an average T of 8.45 keV (dot-dashed line in Figure 3). In this case, the NT flux is $(8.7 \pm 4.2) \times 10^{-12}$ erg cm^{-2} s^{-1} with a decrease of $\sim 33\%$ with respect to the PDS flux due to the smaller HXD-PIN FOV and the higher average temperature. This flux value is consistent with the upper limit of 6×10^{-12} erg cm^{-2} s^{-1} reported by W09 for the NT spectral component with $\Gamma = 2$.

This agreement between the *Suzaku* NT upper limit and the *BeppoSAX* detection has a further confirmation by Figure 8 of Wik et al. (2011) when different spatial models are examined.

We believe that the NT flux of $(1.05 \pm 0.41) \times 10^{-11}$ erg cm^{-2} s^{-1} (see case (1)) cannot be much different from the value measured by W09 for $T = 8.2$ keV, and not reported in their paper (only the c.l. of the excess is in W09), because the flux determined for case (2) is consistent with the *Suzaku* upper limit.

Thus, our SM analysis of the PDS spectrum reproduces the two results present in the W09 analysis: an excess at the c.l. of $\sim 4\sigma$ for an average *XMM-Newton* temperature of 8.2 keV and the upper limit for the NT flux with an average temperature of 8.45 keV obtained by the joint *XMM-Newton*/*Suzaku* analysis. All these reinforce the consistency of the PDS and HXD-PIN spectra and therefore the presence of a hard tail in the Coma cluster spectrum.

4. CONCLUSIONS

For the first time, the HXR spectrum of the Coma cluster has been analyzed using ICP temperature and density profiles instead of considering bremsstrahlung emission for an average temperature in the detector FOVs. These profiles are determined by the SM analysis of X-ray observables. This procedure has allowed us to obtain further checks on the relevant point present in the *Suzaku* analysis that for an *XMM-Newton* temperature $T =$ 8.2 keV reports an NT excess at c.l. $\gtrsim 4\sigma$, which absolutely consistent with the results of FF04 (and therefore in disagreement

with those of RM04). We have shown that the compatibility between the PDS and HXD-PIN spectra has a robust cross-check when in our SM analysis of the PDS data we consider the smaller HXD-PIN FOV and the different average temperatures of 8.2 keV and 8.45 keV (cases (1) and (2), respectively). The agreement between the two spectra is a further confirmation of the presence in the Coma cluster of an NT component. As reported in the previous section, the PDS spectrum gives a hard excess with significance above 4σ also for an ICP average temperature of 8.45 keV. This detection by the PDS is possible thanks to its FOV, a factor of $\sim$4 greater than the HXD-PIN FOV that instead reports a flux upper limit for the same temperature.

We thank Alfonso Cavaliere, Gianfranco Brunetti, Fabio Gastaldello, Francesco Lazzarotto, and Fabio Pizzolato for helpful discussions and our referee for insightful comments, helpful toward improving our presentation. A.L. thanks SISSA for their warm hospitality.

REFERENCES

Ajello, M., Rebusco, P., Cappelluti, N., Reimer, O., Böhringer, H., Greiner, J., Gehrels, N., Tueller, J., & Moretti, A. 2009, ApJ, 690, 367
Ajello, M., et al. 2008, ApJ, 689, 666
Arnaud, M., et al. 2001, A&A, 365, L67
Bautz, M. W., et al. 2009, PASJ, 61, 1117
Bisnovatyi-Kogan, G. S., & Pozanenko, A. S. 2011, Ap&SS, 332, 57
Bonamente, M., Marshall, K. J., & Lieu, R. 2003, ApJ, 585, 722
Bradač, M., et al. 2008, ApJ, 687, 959
Brown, S., & Rudnick, L. 2011, MNRAS, 412, 2
Brunetti, G., Setti, G., Feretti, L., & Giovannini, G. 2001, MNRAS, 320, 365
Castander, F. J., et al. 2001, AJ, 121, 2331
Cavaliere, A., & Lapi, A. 2006, ApJ, 647, L5
Cavaliere, A., Lapi, A., & Fusco-Femiano, R. 2009, ApJ, 698, 580
Cavaliere, A., Lapi, A., & Fusco-Femiano, R. 2011, A&A, 525, 110
Churazov, E., et al. 2007, A&A, 467, 529
Clowe, D., et al. 2006, ApJ, 648, L109
David, L. P., et al. 1993, ApJ, 412, 479
Eckert, D., Neronov, A., Courvoisier, T. J.-L., & Produit, N. 2007, A&A, 470, 835
Ferrari, C., Govoni, F., Schindler, S., Bykov, A. M., & Rephaeli, Y. 2008, Space Sci. Rev., 134, 93
Frontera, F., et al. 2007, ApJ, 666, 86
Fusco-Femiano, R., Cavaliere, A., & Lapi, A. 2009, ApJ, 705, 1019 (FFCL09)
Fusco-Femiano, R., dal Fiume, D., Feretti, L., Giovannini, G., Grandi, P., Matt, G., Molendi, S., & Santangelo, A. 1999, ApJ, 513, L21
Fusco-Femiano, R., Dal Fiume, D., Orlandini, M., Brunetti, G., Feretti, L., & Giovannini, G. 2001, ApJ, 552, L97
Fusco-Femiano, R., Landi, R., & Orlandini, M. 2005, ApJ, 624, L69
Fusco-Femiano, R., Landi, R., & Orlandini, M. 2007, ApJ, 654, L9 (FFLO07)
Fusco-Femiano, R., Orlandini, M., Brunetti, G., Feretti, L., Giovannini, G., Grandi, P., & Setti, G. 2004, ApJ, 602, L73 (FF04)
Fusco-Femiano, R., et al. 2000, ApJ, 534, L7
Gavazzi, R., et al. 2009, A&A, 498, L33
George, M. R., Fabian, A. C., Sanders, J. S., Young, A. J., & Russell, H. R. 2009, MNRAS, 395, 657
Gruber, D. E., Matteson, J. L., Peterson, L. E., & Jung, G. V. 1999, ApJ, 520, 124
Hoshino, A., et al. 2010, PASJ, 62, 371
Hughes, J. P., Butcher, J. A., Stewart, G. C., & Tanaka, Y. 1993, ApJ, 404, 611
Kaastra, J. S., & Mewe, R. 1993, A&AS, 97, 443
Kawaharada, M., et al. 2010, ApJ, 714, 423
Kirsch, M. G., et al. 2005, Proc. SPIE, 5898, 22
Kronberg, P. P., Kothes, R., Salter, C. J., & Perillat, P. 2007, ApJ, 659, 267
Kubo, J. M., et al. 2007, ApJ, 671, 1466
Lapi, A., Cavaliere, A., & Menci, N. 2005, ApJ, 619, 90
Lapi, A., Fusco-Femiano, R., & Cavaliere, A. 2010, A&A, 516, L34
Leccardi, A., Rossetti, M., & Molendi, S. 2010, A&A, 510, A82
Lokas, E. L., & Mamon, G. A. 2003, MNRAS, 343, 401
Lutovinov, A. A., Vikhlinin, A., Churazov, E. M., Revnivtsev, M. G., & Sunyaev, R. A. 2008, ApJ, 687, 968
Mewe, R., Gronenschild, E. H. B. M., & van den Oord, G. H. J. 1985, A&AS, 62, 197
Mewe, R., Lemen, J. R., & van den Oord, G. H. J. 1986, A&AS, 65, 511
Mohr, J. J., Mathiesen, B., & Evrard, A. E. 1999, ApJ, 517, 627
Morrison, R., & McCammon, D. 1983, ApJ, 270, 119
Nakazawa, K., et al. 2009, PASJ, 61, 339
Neumann, D. M., Lumb, D. H., Pratt, G. W., & Briel, U. G. 2003, A&A, 400, 811
Reiprich, T. H., et al. 2009, A&A, 501, 899
Rephaeli, Y. 1979, ApJ, 227, 364
Rephaeli, Y., & Gruber, D. 2002, ApJ, 579, 587
Rephaeli, Y., & Gruber, D. 2003, ApJ, 595, 137
Rephaeli, Y., Gruber, D., & Blanco, P. 1999, ApJ, 511, L21
Rephaeli, Y., Nevalainen, J., Ohashi, T., & Bykov, A. M. 2008, Space Sci. Rev., 134, 71
Ricker, P. M., & Sarazin, C. L. 2001, ApJ, 561, 621
Rossetti, M., & Molendi, S. 2004, A&A, 414, L41 (RM04)
Snowden, S. L., Mushotzky, R. F., Kuntz, K. D., & Davis, D. S. 2008, A&A, 478, 615
Vikhlinin, A, Kravtsov, A., Forman, W., Jones, C., Markevitch, M., Murray, S. S., & Van Speybroeck, L. 2006, ApJ, 640, 691
Wik, D. R., Sarazin, C. L., Finoguenov, A., Baumgartner, W. H., Mushotzky, R. F., Okajima, T., Tueller, J., & Clarke, T. E. 2011, ApJ, 727, 119
Wik, D. R., Sarazin, C. L., Finoguenov, A., Matsushita, K., Nakazawa, K., & Clarke, T. E. 2009, ApJ, 696, 1700 (W09)